

## Variations of low-latitude geomagnetic fields and *Dst* index caused by magnetospheric substorms

Chao-Song Huang,<sup>1</sup> J. C. Foster,<sup>1</sup> L. P. Goncharenko,<sup>1</sup> G. D. Reeves,<sup>2</sup>  
J. L. Chau,<sup>3</sup> K. Yumoto,<sup>4</sup> and K. Kitamura<sup>4</sup>

Received 25 November 2003; revised 24 February 2004; accepted 7 April 2004; published 25 May 2004.

[1] We present observations of periodic magnetospheric substorms and corresponding ionospheric disturbances. Since the periodic substorms occur during a stable interplanetary magnetic field, we are able to identify which ionospheric signatures are caused solely by substorms. We find that the low-latitude ionospheric electric field perturbation after substorm onsets is eastward on the dayside and westward on the nightside and that the ground magnetometer northward ( $H$ ) deviations at middle and low latitudes show an increase (a positive bay) after each substorm onset, no matter whether the magnetometers are located on the dayside or on the nightside. The nightside magnetometer  $H$  deviations are closely correlated with the inner magnetospheric magnetic field  $B_z$  component during the dipolarization process. The *Dst* index shows a significant increase of 20–40 nT after each substorm onset. We propose that the increase in the magnetometer  $H$  field and *Dst* index in response to substorm onsets is related to the field dipolarization. In this scenario the nightside magnetosphere earthward of the near-Earth neutral line is highly compressed during the dipolarization, and the magnetic flux density within the inner magnetosphere is greatly enhanced, resulting in an increase in the ground magnetometer  $H$  component and in *Dst*. **INDEX TERMS:** 2788 Magnetospheric Physics: Storms and substorms; 2740 Magnetospheric Physics: Magnetospheric configuration and dynamics; 2712 Magnetospheric Physics: Electric fields (2411); 2435 Ionosphere: Ionospheric disturbances; **KEYWORDS:** magnetic storms, substorms, dipolarization, geomagnetic disturbances, ionospheric electric field, *Dst* index

**Citation:** Huang, C.-S., J. C. Foster, L. P. Goncharenko, G. D. Reeves, J. L. Chau, K. Yumoto, and K. Kitamura (2004), Variations of low-latitude geomagnetic fields and *Dst* index caused by magnetospheric substorms, *J. Geophys. Res.*, 109, A05219, doi:10.1029/2003JA010334.

### 1. Introduction

[2] The *Dst* index is an important parameter that is a measure of disturbances of the ring current during magnetic storms. The ring current is significantly enhanced during storm times, and the westward ring current decreases the northward component of the Earth's surface magnetic field. Substorms often occur while magnetic storms are developing, and energetic plasma particles are injected from the tail into the inner magnetosphere after substorm onsets. It is generally expected that the newly injected particles increase the ring current and cause a decrease in the geomagnetic field  $H$  component and in the *Dst* index. However, observations show results that are contradictory to the expected *Dst* change. *Iyemori and Rao* [1996] investigated the temporal evolution of the 1-min resolution SYM- $H$  and

ASY- $H$  indices in association with substorms. SYM- $H$  is essentially a higher-resolution version of *Dst* and a measure of the symmetric component of the ring current, and ASY- $H$  is interpreted as the asymmetric component of the ring current. In the main phase of storms the time rate of decrease of *Dst* slows after substorm onsets. In the recovery phase of storms *Dst* even increases (becomes less negative) after the onsets. *Siscoe and Petschek* [1997] used the generalized virial theorem to explain the observations of *Iyemori and Rao* [1996].

[3] *McPherron* [1997] demonstrated that most of the variance in *Dst* is caused by the solar wind. Ring current injection can be directly driven by the solar wind, and *Dst* starts to decrease at the beginning of the substorm growth phase. Although the substorm expansion phase alone makes *Dst* become less negative, *Dst* will decrease over an entire substorm process, from the beginning of the growth phase to after the expansion phase. The simulations of *Ebihara and Ejiri* [2000] also show that the major variation of storm time *Dst* is mainly due to the changes in the magnetospheric convection electric field and plasma sheet plasma density.

[4] The tail current may play a significant role in the *Dst* variations during substorms [*Iyemori and Rao*, 1996; *Alexeev et al.*, 1996; *Maltsev et al.*, 1996]. *Turner et al.* [2000] used the Tsyganenko magnetic field models to calculate the contribution of the tail current to *Dst*. The tail

<sup>1</sup>Haystack Observatory, Massachusetts Institute of Technology, Westford, Massachusetts, USA.

<sup>2</sup>Los Alamos National Laboratory, Los Alamos, New Mexico, USA.

<sup>3</sup>Radio Observatorio de Jicamarca, Instituto Geofísico del Perú, Lima, Perú.

<sup>4</sup>Space Environment Research Center, Kyushu University, Fukuoka, Japan.

current intensification during the growth phase of storm time substorms can contribute 22–26 nT to the *Dst* index. Because the tail current is disrupted at the substorm onset, the contribution to *Dst* from the tail current becomes less important. Therefore *Dst* will show an increase after the expansion onset. *Reeves et al.* [2003] concluded that the increases in the *Dst* and SYM-*H* indices after substorm onsets are related to the dipolarization.

[5] The *Dst* index is derived from ground magnetometer measurements at middle latitudes. Ionospheric signatures of substorms at middle and low latitudes were studied using radar and magnetometer data. *Sibeck et al.* [1998] have shown that about one third of the northward equatorial magnetic field variations are associated with variations in the solar wind pressure, a second third with substorm onsets, and the final third with interplanetary magnetic field (IMF) reorientations in the north-south direction. *Fejer et al.* [1979], *Gonzales et al.* [1979], and *Kelley et al.* [1979] found that equatorial ionospheric electric field perturbations at substorm onsets were westward on the dayside and eastward on the nightside. The ground magnetometer deviations at substorm onsets were attributed to the variations in the ring current. The substorm onsets in their cases were coincident with northward reversals of the IMF. *Kikuchi et al.* [2000] and *Sastri et al.* [2001] found that the dayside magnetometer *H* component at middle and low latitudes showed a decrease (a negative bay) after substorm onsets. *Sastri et al.* [2001] also reported on an event in which a positive bay occurred in the *H* component of low-latitude magnetometers during the substorm expansion phase. They thought that the occurrence of the positive bay was “rather puzzling.”

[6] The expansion onsets of isolated substorms are often correlated with northward IMF turnings [*McPherron et al.*, 1986]. IMF turnings in the north-south direction cause electric field perturbations in the ionosphere through penetration of the interplanetary electric field (IEF), no matter whether the IMF turnings trigger substorm onsets. There have been extensive studies of IEF penetration into the middle- and low-latitude ionosphere [*Nishida*, 1968; *Blanc*, 1983; *Fejer et al.*, 1990; *Buonsanto et al.*, 1999; *Kikuchi et al.*, 2001; *Huang and Foster*, 2001; *Huang et al.*, 2002; *Kelley et al.*, 2003]. If the IMF turns from southward to northward, the ionospheric electric field perturbation is westward on the dayside. Such a westward electric field will cause a decrease of the ground magnetometer *H* component at the equator.

[7] A number of significant issues associated with low-latitude ionospheric signatures of substorms are not well understood. As mentioned above, it was reported that a negative bay of the dayside magnetometer *H* component was coincident with the substorm onsets [*Kikuchi et al.*, 2000; *Sastri et al.*, 2001]. However, it is not clear whether the negative bay was caused by a substorm onset or by a northward IMF turning that triggered the substorm onset. This question is answered in part by *Kikuchi et al.* [2003]. They found that a northward turning of the IMF resulted in a decrease in the polar cap potential and equatorial magnetic *H* component, suggesting that a westward electric field penetrated into the equatorial ionosphere. Another question is how the ionospheric electric field varies in response to substorm onsets without coincident IMF northward turn-

ings. Furthermore, the *Dst* index is derived from ground magnetometers. A detailed comparison between magnetospheric and ionospheric disturbances is helpful for identifying the mechanisms that can cause the *Dst* increases at substorm onsets during storms.

[8] In order to study the magnetospheric-ionospheric disturbances caused by substorms alone, it is necessary to exclude the effects of IMF northward turnings. Recently, there has been great interest in periodic substorms during storm times [*Huang*, 2002; *Huang et al.*, 2003a, 2003b, 2003c; *Reeves et al.*, 2003; *Kitamura et al.*, 2003]. A prominent feature of these observations is that substorms with a clear period of 2–3 hours occur and last for 6–10 cycles during persistent southward IMF. Because the IMF and solar wind pressure are stable, the periodic onsets of substorms must be related to some internal processes in the magnetosphere. *Huang et al.* [2003c] suggest that substorms have an intrinsic cycle time of 2–3 hours, and the period of substorms is determined by the magnetosphere. Each cycle of the periodic substorms does not have to be triggered by either a northward IMF turning or by a solar wind pressure impulse.

[9] In this paper, we use space-based and ground-based instrumental measurements to study ionospheric electric and magnetic field perturbations associated with substorms. In particular, we will investigate substorm occurrence under stable solar wind conditions. Our purpose is to identify which ionospheric signatures are caused solely by solar wind variations and which are caused solely by magnetospheric substorms. On the basis of our observations we will propose an interpretation of the increases in *Dst* at substorm onsets.

## 2. Observations and Interpretation

[10] We present in Figure 1 the *Dst* and SYM-*H* indices during the magnetic storm of 17–18 April 2002. A sudden storm commencement occurred at 1109 UT on 17 April, and *Dst*/SYM-*H* reached a minimum value around 0800 UT on 18 April. The two indices are in good agreement. *Dst* has a time resolution of 1 hour, and SYM-*H* has a time resolution of 1 min [*Iyemori and Rao*, 1996, and references therein]. SYM-*H* is essentially a higher-resolution version of *Dst*. Since the substorm expansion phase lasts only for 10–60 min, *Dst* is not a suitable parameter for studying the rapid variations caused by substorm onsets. In the following, we will mainly use the SYM-*H* data for our analyses. We treat *Dst* and SYM-*H* as the same parameter with different time resolutions and write it as *Dst*/SYM-*H* in the text. In Figure 1 the vertical dotted lines are used to indicate the times of substorm onsets, which are identified from geosynchronous particle injections and will be discussed in detail later. A remarkable feature is that *Dst*/SYM-*H* shows a sudden increase at each substorm onset during both the main phase and the recovery phase of the storm, and the increase in *Dst*/SYM-*H* is as high as 20–40 nT.

[11] We first study an isolated substorm at nonstorm times before we conduct detailed analyses of periodic substorms during storm times. Figure 2a shows the solar wind dynamic pressure, IMF  $B_z$  component, and IEF  $E_y$  component measured by the Wind satellite at about  $X_{\text{GSM}} = 58 R_E$  on 13 April 2000. The solar wind at a velocity of  $375 \text{ m s}^{-1}$

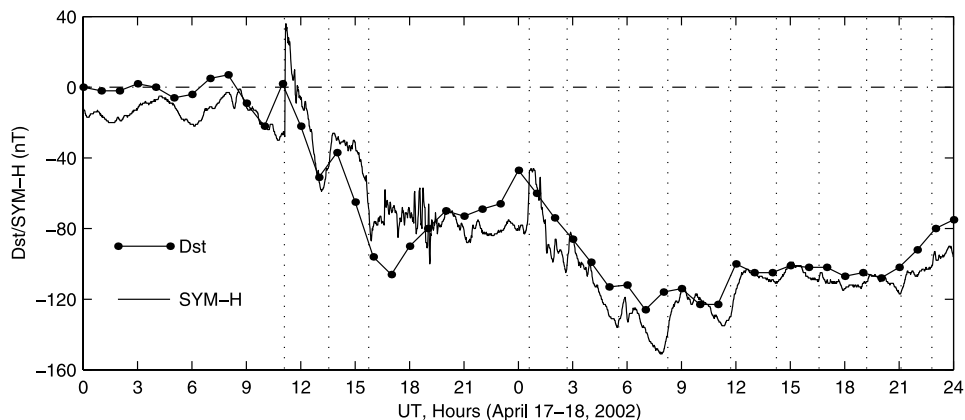


**Figure 1.** *Dst* and *SYM-H* indices during 17–18 April 2002. The vertical dotted lines indicate substorm onsets.

would take  $\sim 12$  min to travel from the Wind position to the bow shock and an additional  $\sim 5$  min to travel through the magnetosheath. Accordingly, the solar wind data have been shifted by 17 min in Figure 2a. Figure 2b shows the auroral electrojet (AE) index. A sudden increase in AE occurs at 0305 UT, indicating the onset of a substorm. The minimum *Dst* value is  $-29$  nT on this day, so this substorm is classified as one at nonstorm times. The IMF  $B_z$  shows an increase in the northward direction or becomes less negative after 0305 UT. A less southward IMF will cause a reduction in the convection electric field, and the substorm onset might be related to the incomplete northward turning of the IMF [Lyons, 1995]. Figure 2c shows the nightside equatorial ionospheric response to the substorm. The east-west ionospheric electric field  $E_y$ , which is averaged over the altitude range of 248–548 km, measured by the Jicamarca

incoherent radar, becomes less negative after 0305 UT ( $\sim 2205$  magnetic local time (MLT)) but does not change to positive (eastward). The northward ( $H$ ) component of the ground magnetometer at Jicamarca increases by  $\sim 20$  nT following the substorm onset. Figure 2d shows the dayside variations of the  $H$  component measured by the Solar-Terrestrial Energy Program (STEP) 210 (degree) magnetic meridian chain around geographic longitudes  $110^\circ$ – $140^\circ$  [Yumoto *et al.*, 2001], and a clear increase occurs at 0305 UT ( $\sim 1200$  MLT). The locations of the ground magnetometers are listed in Table 1.

[12] A very important feature in this case is that the ionospheric response to the substorm onset is an increase in the  $H$  component of the ground magnetometers on both the dayside and the nightside and continuous westward equatorial electric field on the nightside. The slight decrease

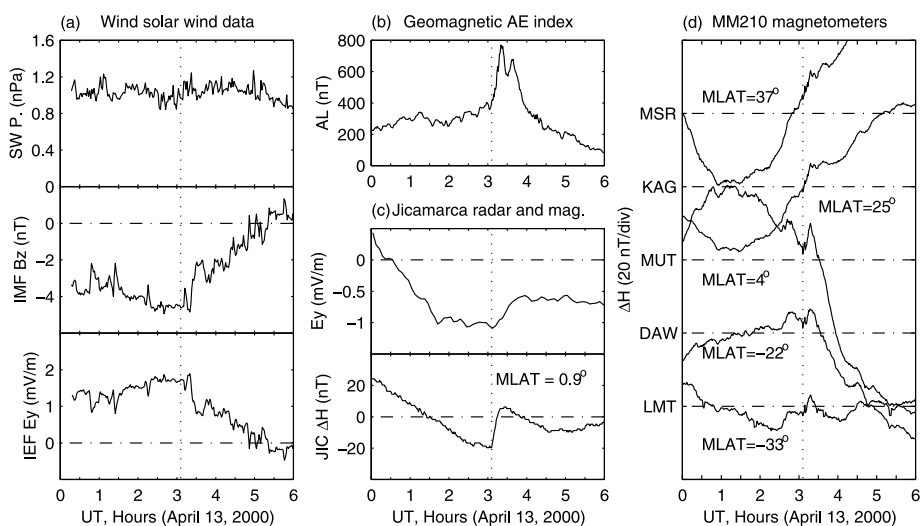


**Figure 2.** (a) Solar wind pressure, interplanetary magnetic field (IMF)  $B_z$  component, and interplanetary electric field (IEF)  $E_y$  component measured by the Wind satellite. (b) Auroral electrojet (AE) index. (c) Nightside equatorial ionospheric electric field  $E_y$ , measured by the Jicamarca radar and deviations of the northward ( $H$ ) component of the ground magnetometer at Jicamarca (MLT = UT – 5 hours). (d) Dayside deviations of the  $H$  component of the STEP magnetometers at Moshiri (MSR), Kogoshima (KAG), Muntinlupa (MUT), Darwin (DAW), and Learmonth (LMT) along magnetic longitude  $\sim 210^\circ$  (MLT = UT + 9 hours) on 13 April 2000. Magnetic latitude (MLAT) for each station is given in the plot. The vertical dotted line indicates the onset of a substorm.

**Table 1.** Locations of Ground Magnetometers

Station	Abbreviation	Geographic		Geomagnetic	
		Longitude	Latitude	Longitude	Latitude
<i>Jicamarca Magnetometers</i>					
Jicamarca	JIC	283.1	-11.9	-5.2	0.9
Piura	PIU	279.3	-5.2	-9.1	7.1
<i>STEP 210 (deg) Magnetometers</i>					
Moshiri	MSR	142.2	44.3	213.3	37.6
Kogoshima	KAG	130.7	31.4	202.3	24.3
Muntinlupa	MUT	121.0	14.3	192.2	6.3
Weipa	WEP	141.8	-12.6	214.4	-21.9
Darwin	DAW	130.9	-12.4	202.7	-22.0
Learmonth	LMT	114.1	-22.2	185.1	-33.5
Canberra	CAN	149.0	-35.3	226.2	-45.9

in the magnitude of the nightside westward electric field at Jicamarca is very likely to be associated with the gradual decrease of the IMF  $B_z$  magnitude after 0305 UT. In previous studies, low-latitude ionospheric response to substorm onsets was described as an eastward electric field perturbation on the nightside [Fejer *et al.*, 1979; Gonzales *et al.*, 1979] and a decrease in the ground magnetometer  $H$  component on the dayside [Kikuchi *et al.*, 2000; Sastri *et al.*, 2001]. However, the substorm onsets in the previous observations were related to IMF northward turnings. We will discuss the interpretation of the ionospheric signatures of substorms and will address the importance of separating the IMF turning and substorm effects after we present the measurements of periodic substorms during a long interval (up to 24 hours) of persistent southward IMF.

[13] We now turn to periodic substorms during storm times. Figure 3a depicts the solar wind data measured by the Wind satellite at  $X_{\text{GSM}} = 12 R_E$  on 17 April 2002; the  $Dst$  data on this day are displayed in Figure 1. The Wind data are shifted by 6 min to the right to allow for the solar wind propagation from the satellite position to the magnetosphere. In the shifted data the solar wind pressure jumps from 4.1 nPa at 1105 UT to 23.5 nPa at 1109 UT, and this solar wind pressure impulse may have caused the storm sudden commencement. The IMF  $B_z$  component changes several times between southward and northward, and the IEF  $E_y$  component, which is calculated from the  $X$ -directed solar wind velocity and IMF  $B_z$ , changes between duskward (positive) and dawnward (negative). The vertical dashed lines at 1230, 1415, 1540, 1645, and 1833 UT indicate the negative peaks in the IMF  $B_z$  and positive peaks in the IEF  $E_y$ .

[14] Figure 3b presents the energetic electron fluxes measured by the Los Alamos National Laboratory (LANL) 1994-084 satellite at geosynchronous orbit; magnetic local time (MLT) at 1994-084 is UT plus 9.5 hours. LANL 1994-084 is on the nightside during the period of interest; its measurements can provide an accurate timing of substorm onsets because energetic plasma particles are injected from the magnetotail in the inner magnetosphere near midnight during the expansion phase of substorms. Three vertical dotted lines are used to indicate sudden increases in the electron fluxes. The first flux increase at 1106 UT is related to the solar wind pressure impulse. As discussed by Huang *et al.* [2003b, 2003c], sawtooth substorm injections at geosynchronous orbit are characterized by a gradual decrease during the growth phase of substorms and a

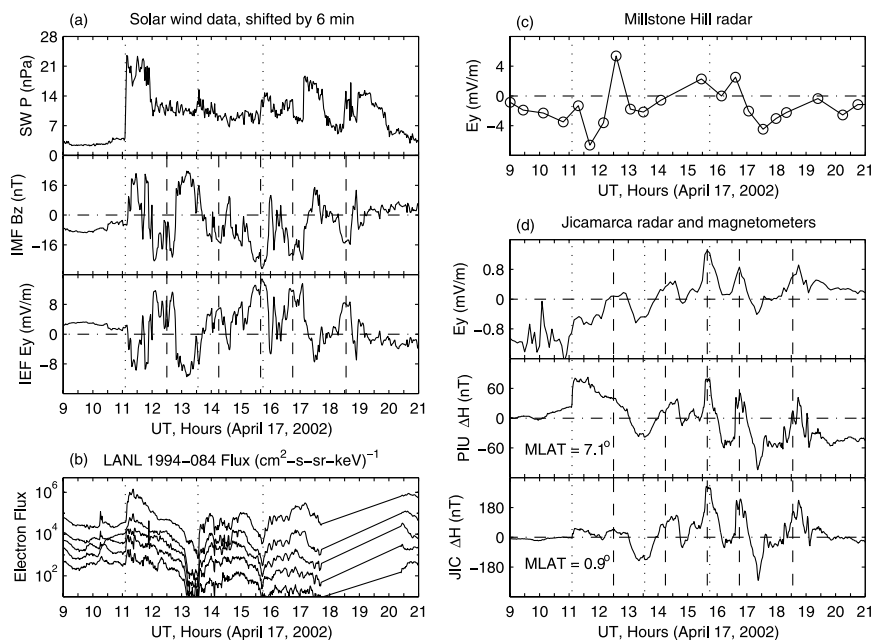


**Figure 3.** (a) Solar wind pressure, IMF  $B_z$ , and IEF  $E_y$  measured by the Wind satellite on 17 April 2002. The vertical dashed lines indicate negative peaks in the IMF  $B_z$  and positive peaks in the IEF  $E_y$ . (b) Energetic electron fluxes at geosynchronous orbit. The energy channels of the electron fluxes, from top to bottom, are 50–75, 75–105, 105–150, 150–225, and 225–315 keV. The vertical dotted lines indicate substorm onsets. (c) Midlatitude ionospheric electric field  $E_y$  measured by the Millstone Hill radar. (d) Equatorial ionospheric electric field  $E_y$  measured by the Jicamarca radar and deviations of the northward ( $H$ ) component of ground magnetometers at Piura (PIU) and Jicamarca (JIC).



sudden increase at the expansion onset. The vertical dotted lines at 1333 and 1545 UT indicate substorm onsets which are coincident with two relatively smaller solar wind pressure impulses. The solar wind pressure increases from 10.1 nPa at 1328 UT to 15.5 nPa at 1335 UT and from 7.3 nPa at 1536 UT to 14.7 nPa at 1548 UT, and these solar wind pressure impulses may have triggered the two substorm onsets. It is important to note that the IEF  $E_y$  changes from negative to positive after the first substorm onset at 1333 UT and from positive to negative after the second substorm onset at 1545 UT. The change in the IEF has direct effects on the dayside ionospheric electric and magnetic fields.

[15] The measurements of ionospheric electric fields on 17 April 2002 are shown in Figures 3c and 3d. The Millstone Hill radar was operated in a 5-position mode to measure three-dimensional  $F$  region ion velocities (electric fields) and meridional neutral winds. The 5-position radar mode includes three positions of the steerable antenna with a fixed elevation angle of  $45^\circ$ , one position of the steerable antenna along the magnetic field line, and the fixed vertically directed position of the zenith antenna [Buonsanto and Holt, 1995]. The cycle time of the steerable antenna was  $\sim 30$  min in this experiment. The time resolution of the Jicamarca radar data was 5 min, and the electric field data in Figure 3d are averaged over the altitude range of 330–495 km. The ionospheric electric field  $E_y$  is defined as positive in the eastward direction and negative in the westward direction. The positive peaks of the ionospheric electric field at 1230, 1415, 1540, 1645, and 1833 UT, as marked by the vertical dashed lines, correspond well to the peaks in the IEF  $E_y$  presented in Figure 3a, indicating the penetration of the interplanetary electric field into the ionosphere [Kelley *et al.*, 2003]. MLT is about UT minus 5 hours at both the Millstone Hill and Jicamarca radar sites. Also shown in Figure 3d are the deviations of the  $H$  component of the ground magnetometers at Piura and Jicamarca. There is a one-to-one correspondence between the electric field perturbations and magnetometer  $H$  deviations. The amplitude of the  $H$  deviations at Jicamarca is much larger than that at Piura. Since the Jicamarca magnetometer is closer to the magnetic dip equator, the larger magnetic deviations nearer to the equator are clearly related to the equatorial electrojet which is enhanced by the eastward electric field through the Cowling effect [Anderson *et al.*, 2002].

[16] The  $H$  deviations change from negative to positive after the onset at 1333 UT but from positive to negative after the onset at 1545 UT. The opposite polarity of the  $H$  deviations is caused by the electric field perturbations but not by the substorm onsets. The ionospheric electric field changes from negative to positive after 1333 UT and from positive to negative after 1545 UT. In the dayside equatorial ionosphere the conductivity is large, and the  $E$  region current is mainly the Pedersen current. Electric field and current perturbations in the east-west direction produce magnetic deviations in the north-south direction. The important implication of the observations in this case is that the dayside magnetometer deviations at substorm onsets may be determined primarily by the ionospheric electric field perturbation that is the penetration of the interplanetary electric field if the IMF changes direction. In particular, the

onsets of isolated substorms are often triggered by a northward IMF turning that corresponds to the turning of the interplanetary electric field from duskward to dawnward. The dayside ionospheric electric field will change from eastward to westward, resulting in a decrease (or negative bay) in the magnetometer  $H$  component. In contrast, the dayside magnetometer  $H$  component deviation is positive at the substorm onset when the IMF  $B_z$  remains southward, as shown in Figure 2.

[17] In order to exclude the effects of the penetration electric field, it is desirable to choose intervals of stable IMF. Figure 4 presents such an example. A storm sudden commencement occurred at 1648 UT on 22 October 2001, and SYM- $H$  reached a minimum value of  $-219$  nT at 2129 UT and took 3 days to recover. The substorms we are studying occurred during the initial recovery phase of the storm. In Figure 4a the solar wind data measured by the Wind satellite at  $X_{\text{GSM}} = 25 R_E$  have been shifted by 7 min to the right. The solar wind could take 2 min to travel from the Wind position to the bow shock and an additional 5 min to travel through the magnetosheath. The solar wind pressure impulse around 1700 UT corresponds well to a compression of the dayside magnetosphere after the 7-min shift. In Figure 4b the counts of energetic particles measured by the LANL 1991-080 geosynchronous satellite are plotted, and the vertical dotted lines at 1112, 1330, 1600, and 1809 UT indicate substorm onsets. In Figure 4c the SYM- $H$  index is displayed. The substorm onsets occur without IMF northward turnings, and the SYM- $H$  increases (becomes less negative) after each substorm onset.

[18] The dayside ionospheric response to the substorms on 22 October 2001 is presented in Figure 4d. In this experiment, the equatorial  $F$  region  $\mathbf{E} \times \mathbf{B}$  drifts were measured by the Jicamarca radar from the Doppler shifts of the so-called “150-km” echoes. Although there is no good understanding of the mechanisms generating 150-km echoes, they are very strong and come from field-aligned irregularities [e.g., Kudaki and Fawcett, 1993]. A prominent feature in Figure 4d is that the ionospheric electric field shows two large enhancements at the substorm onsets at 1600 and 1809 UT. As can be seen in Figure 4a, there is a decrease from  $-6.5$  nT at 1559 UT to  $-10.3$  nT at 1609 UT in the IMF  $B_z$ , and the corresponding IEF  $E_y$  changes from  $3.5$  to  $5.5$   $\text{mV m}^{-1}$ . According to Kelley *et al.* [2003], the ratio of the dawn-dusk component of the IEF to the east-west penetration electric field in the dayside equatorial ionosphere is  $\sim 7\%$ . The change of  $2$   $\text{mV m}^{-1}$  in the IEF  $E_y$  may cause a change of  $\sim 0.14$   $\text{mV m}^{-1}$  in the equatorial electric field. However, the measured ionospheric electric field changes from  $0.19$   $\text{mV m}^{-1}$  at 1602 UT to  $0.72$   $\text{mV m}^{-1}$  at 1617 UT, and the increase of  $0.53$   $\text{mV m}^{-1}$  cannot be attributed to the penetration interplanetary electric field. Furthermore, the ionospheric electric field shows another peak after the onset at 1809 UT, while there is no change in the IMF  $B_z$  at this moment. Therefore we suggest that the increases of the dayside eastward ionospheric electric field at 1600 and 1809 UT (1100 and 1309 MLT) are caused by the corresponding substorm onsets. The ground magnetometers show variations similar to the electric field. The  $H$  deviation at Jicamarca is much larger than that at Piura, again indicating the enhancement of the equatorial electrojet by the eastward electric field perturbation through the

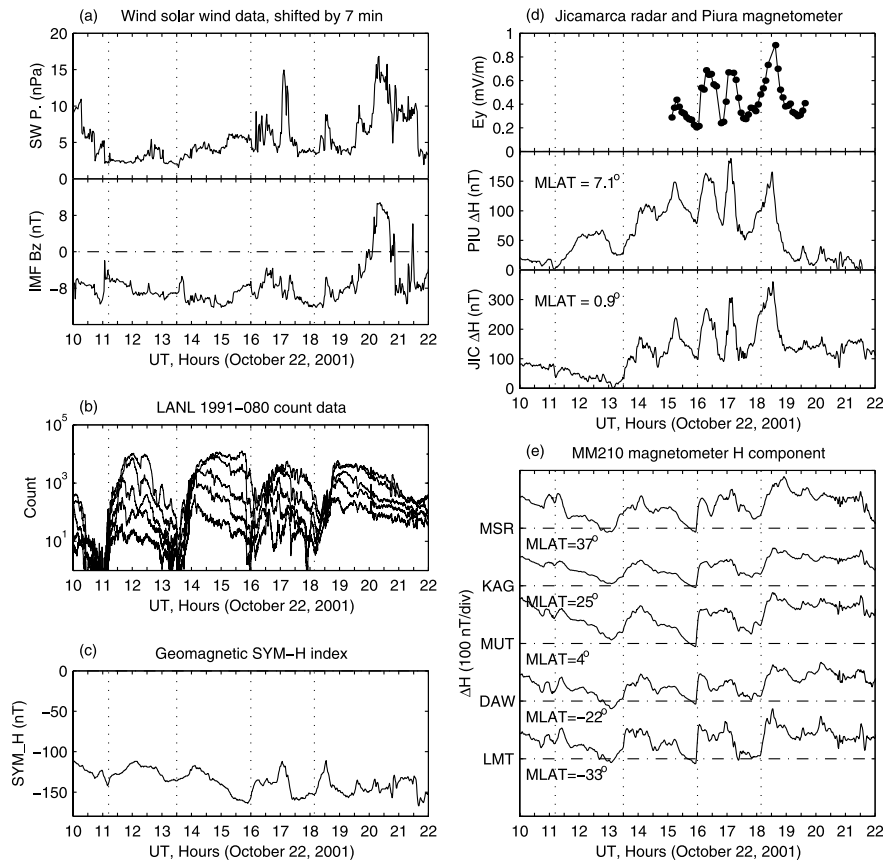


**Figure 4.** (a) Solar wind pressure and IMF  $B_z$  measured by the Wind satellite on 22 October 2001. (b) Counts of energetic particles measured by the LANL 1991-080 satellite. The vertical dotted lines indicate substorm onsets. (c) SYM- $H$  index. (d) Equatorial ionospheric electric field  $E_y$ , measured by the Jicamarca radar and deviations of the magnetometer  $H$  component at Piura and Jicamarca. (e) Deviations of the  $H$  component of the STEP magnetometers at MSR, KAG, MUT, DAW, and LMT.

Cowling effect. The  $H$  deviation also increases after the substorm onsets at 1112 and 1330 UT. Because of the one-to-one correspondence between the electric field and magnetometer perturbations we expect that an eastward electric field perturbation also exists at 1112 and 1330 UT. The impulse in the ionospheric electric field and magnetometer  $H$  deviations at 1700 UT is related to a solar wind pressure impulse (Figure 4a) and is not a signature of the substorms.

[19] We take a look at the nightside magnetometer response to the substorms in this case. Figure 4e shows the deviations of the  $H$  component measured by the STEP magnetic meridian magnetometer chain. The magnetometers from the southern to northern hemispheres all show a sudden increase after each substorm onset. The nightside magnetometer increases in response to the substorm onsets are not determined by the electric field perturbations. If magnetospheric electric fields penetrate into the ionosphere, the electric fields in the low-latitude ionosphere will have opposite directions on the different sides of the Earth. That is, the ionospheric electric field will be eastward on the dayside and westward on the nightside and vice versa. Figure 4d shows that the ionospheric electric field perturbation after the substorm onsets is eastward on the dayside, and thus the electric field perturbation in the nightside ionosphere should be westward. A westward electric field

would cause a negative (southward) deviation in the magnetometer  $H$  component. However, the measured  $H$  deviations are positive. In fact, the nightside ionospheric conductivity at low latitudes is very low (about 20 times smaller than the dayside conductivity) near midnight and postmidnight, and the electric field is unlikely to produce any significant deviations in the magnetometers. The nightside magnetometer  $H$  deviations must be caused by some mechanisms other than ionospheric electric fields. The magnetometer  $H$  response to the substorm onsets in this case is an increase on both the dayside and nightside, the same as in the case of the isolated substorm without IMF northward turning (Figure 2).

[20] As shown in Figure 4d, the ionospheric electric field perturbation after substorm onsets is eastward on the dayside, so the expected nightside electric field perturbation is westward. We present an example of the measurements of nightside electric fields. Figure 5a shows the solar wind pressure and IMF  $B_z$  measured by the Wind satellite near the Earth on 18 April 2001. A sudden increase in the solar wind pressure occurs at 0047 UT. In this case, we use the magnetic elevation angle in the inner magnetosphere to indicate the onsets of substorms. The magnetospheric magnetic field is highly stretched during the growth phase of substorms and suddenly becomes more dipolar after the

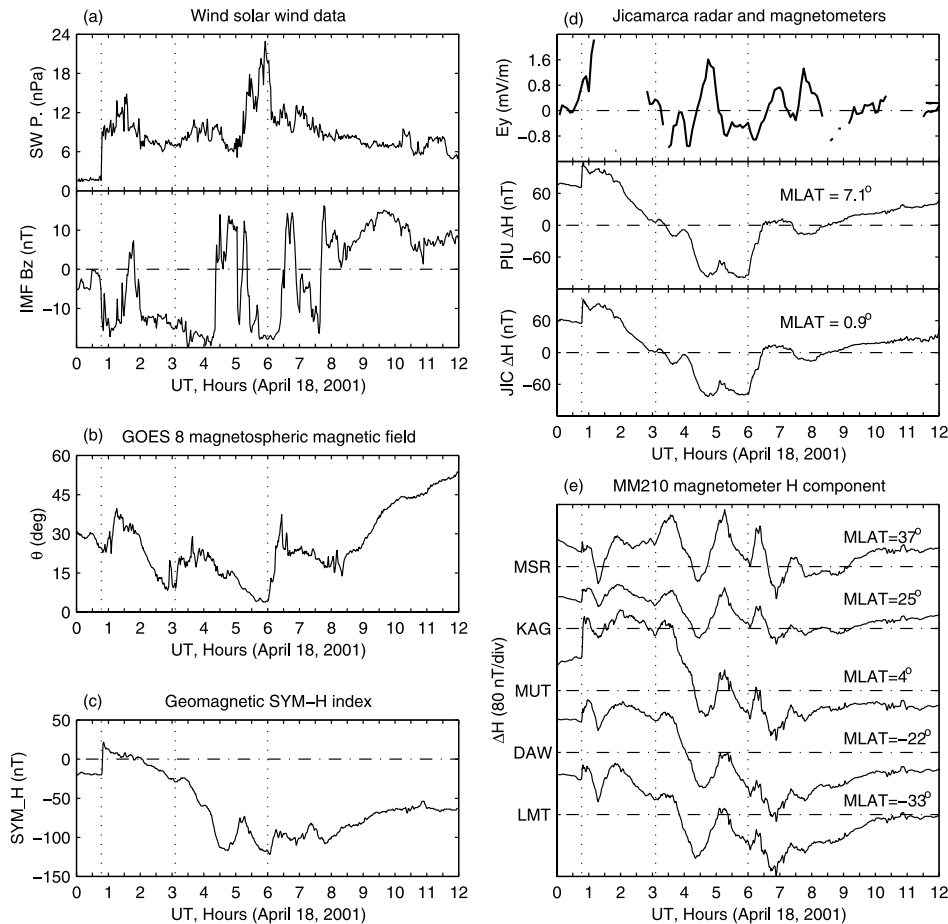


**Figure 5.** (a) Solar wind pressure and IMF  $B_z$  measured by Wind on 18 April 2001. (b) Magnetospheric magnetic field elevation angle measured by GOES 8. The vertical dotted lines indicate substorm onsets. (c) SYM- $H$  index. (d) Equatorial ionospheric electric field  $E_y$ , measured by the Jicamarca radar and deviations of the magnetometer  $H$  component at Piura and Jicamarca. (e) Deviations of the  $H$  component of the STEP magnetometers at MSR, KAG, MUT, DAW, and LMT.

onset. The dipolarization is the signature of a dramatic reconfiguration of the magnetosphere during substorms and is characterized by the magnetic field elevation in the plasma sheet [Baumjohann *et al.*, 1999; Huang *et al.*, 2003b]. The elevation angle is defined as  $\tan^{-1}[B_z/(B_x^2 + B_y^2)^{1/2}]$ . Figure 5b shows the elevation angle measured by the geosynchronous GOES 8 satellite (MLT = UT - 5 hours). Two sudden increases of the elevation angle occur at 0306 and 0600 UT near local midnight. We checked energetic particle injections at geosynchronous orbit, and the injections occur at the same times as the dipolarization. In Figure 5c a storm sudden commencement occurs at 0047 UT and is coincident with the solar wind pressure impulse. SYM- $H$  increases after each substorm onset. The IMF  $B_z$  does not show any significant changes at the times of the substorm onsets in this case. The peak in SYM- $H$  at 0516 UT may be related to the solar wind pressure enhancement after 0500 UT. However, it is not clear why a larger enhancement of the solar wind pressure peak at 0555 UT does not cause corresponding changes in SYM- $H$ .

[21] In Figure 5d we plot the nightside equatorial ionospheric electric field  $E_y$  component averaged over the altitude range of 300–500 km and the  $H$  deviations of the

Piura and Jicamarca magnetometers. The electric field measurements have a time resolution of 5 min and some data gaps. The sudden increase in the magnetometer  $H$  deviations at 0047 UT is related to the solar wind pressure impulse, and two other increases in the  $H$  deviations at 0306 and 0600 UT ( $\sim$ 2200 and 0100 MLT) are coincident with the substorm onsets. There are several important features in this case. (1) A westward electric field perturbation occurs after each substorm onset, which is consistent with the eastward electric field perturbation on the dayside. (2) There are three positive peaks in the electric field at  $\sim$ 0440,  $\sim$ 0650, and  $\sim$ 0740 UT, and these peaks are related to the corresponding northward turnings of the IMF shown in Figure 5a but are not caused by the substorm onsets. Ionospheric electric field perturbations caused by northward IMF turnings are westward on the dayside and eastward on the nightside; such IMF-induced ionospheric electric field perturbations are also clear in Figure 3. (3) The magnetometer  $H$  deviations increase after each substorm onset and are not related to the substorm-induced westward electric field perturbation. The westward electric field perturbation would cause, if any, a decrease in the magnetometer  $H$  component. The IMF-induced eastward electric field perturbations at

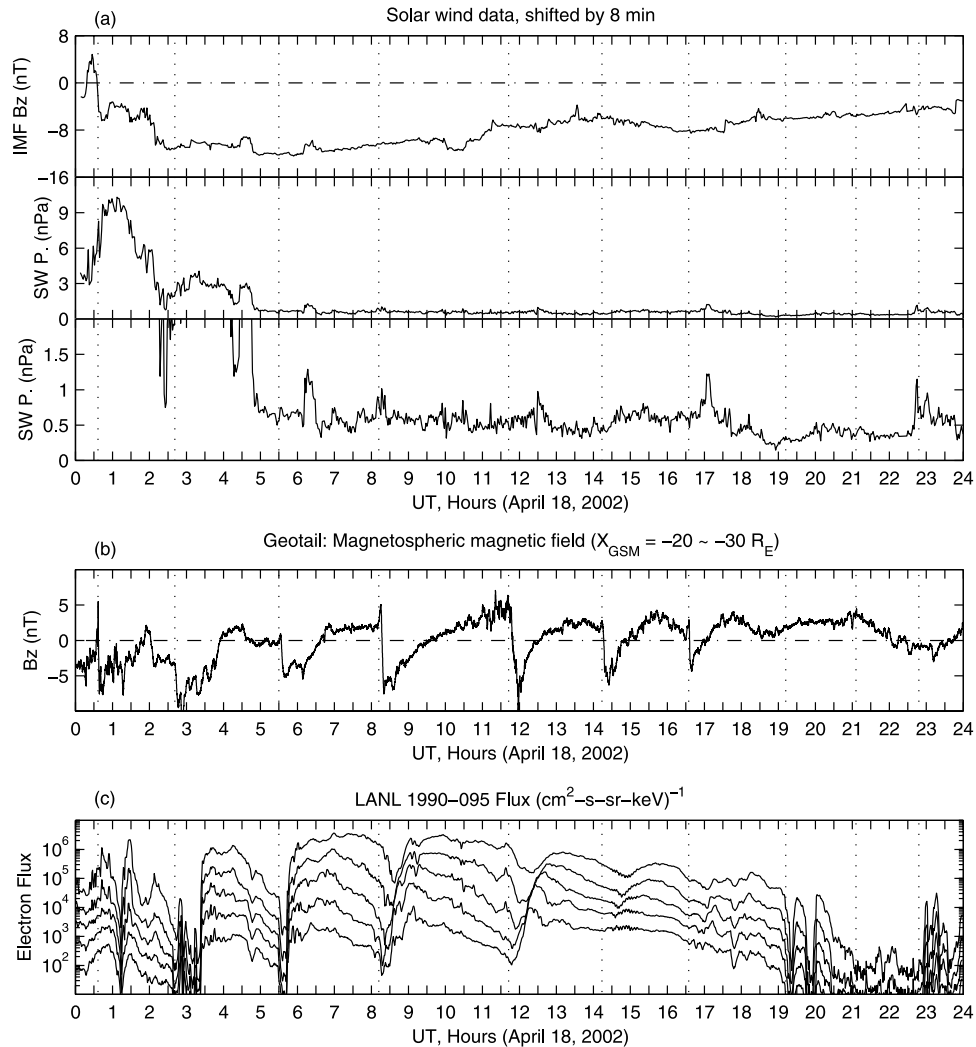


**Figure 6.** (a) IMF  $B_z$  and solar wind pressure measured by Wind, (b) magnetospheric magnetic field  $B_z$  component measured by Geotail, and (c) energetic electron fluxes at geosynchronous orbit on 18 April 2002. The vertical dotted lines indicate substorm onsets.

~0440, ~0650, and ~0740 UT do not produce significant changes in the magnetometers, too. This is because the conductivity is very low in the nightside ionosphere. In addition, the amplitude of the magnetometer  $H$  deviations is almost the same at Piura and Jicamarca, further indicating that there is no electrojet enhancement by the electric field. (4) The nightside magnetometer  $H$  deviations after the substorm onsets have the same trend as the magnetospheric magnetic field  $B_z$  component (or elevation angle). The GOES 8 satellite and Jicamarca magnetometers are at the same local time sector (MLT = UT - 5 hours). The similar variations suggest that the ground magnetometer variations may be related to the magnetospheric dipolarization process at substorm onsets.

[22] During the expansion phase of substorms the cross-tail current is disrupted and diverted along magnetic field lines into the ionospheric auroral oval, forming the so-called “substorm current wedge.” It was suggested that the current wedge might cause a positive bay in the nightside midlatitude magnetometer  $H$  component and a decrease in the dayside midlatitude magnetometer  $H$  component [e.g.,

Clauer and McPherron, 1974]. However, as shown in this paper, the  $H$  component of ground magnetometers at midlatitudes increases on both the dayside and the nightside in response to substorm onsets. The substorm current wedge alone cannot explain how a positive bay also occurs in the dayside midlatitude magnetometers.

[23] The dayside magnetic field  $H$  deviations measured by the STEP magnetometer chain on 18 April 2001 are displayed in Figure 5e. The sudden increase at 0047 UT is related to the solar wind pressure impulse. The increases in the  $H$  deviations at 0306 and 0600 UT (~1200 and 1500 MLT) are the response to the substorm onsets. As shown in Figure 5d, the ionospheric electric field perturbation associated with the substorm onsets is negative (westward) on the nightside, so the dayside ionospheric electric field perturbation should be eastward. An eastward electric field will produce a positive (northward)  $H$  deviation through the Pedersen current. The magnetic signature of Figure 5e is consistent with the electric field measurement in Figure 5d and is also consistent with the measurements in Figure 4 in which both the dayside ionospheric electric



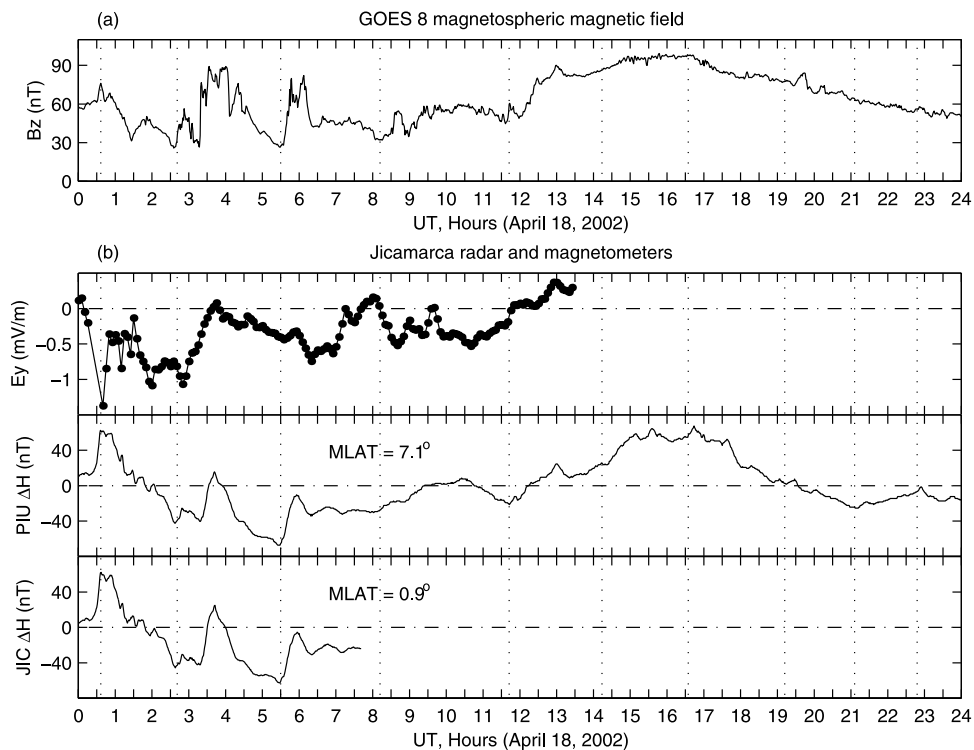


**Figure 7.** (a) Magnetospheric magnetic field  $B_z$  component measured by GOES 8 and (b) equatorial ionospheric electric field  $E_y$  measured by the Jicamarca radar and deviations of the  $H$  component of ground magnetometers at Piura and Jicamarca on 18 April 2002.

field and  $H$  deviations are positive after substorm onsets. The three negative peaks of the dayside magnetometer  $H$  deviations at  $\sim 0440$ ,  $\sim 0650$ , and  $\sim 0740$  UT ( $\sim 1340$ ,  $1550$ , and  $1640$  MLT) in Figure 5e are related to the corresponding IMF northward turnings, and penetration of the interplanetary electric field results in westward electric field perturbations in the dayside ionosphere and negative deviations in the magnetometer  $H$  component. When the IMF reorientates, the convection electric field change is transferred to the auroral ionosphere by the field-aligned currents and is transmitted to the middle- and low-latitude ionosphere; this process has been investigated in detail by Kikuchi *et al.* [2000, 2001, 2003].

[24] We have presented the  $Dst$  and SYM- $H$  data of 17–18 April 2002 in Figure 1 and the magnetospheric-ionospheric measurements of 17 April 2002 in Figure 3. We now take a closer look at the data of 18 April 2002. Figure 6a shows the IMF  $B_z$  and solar wind pressure measured by the Wind satellite; Figure 6b shows the magnetospheric magnetic field  $B_z$  component measured by the Geotail satellite in the tail between  $-20$  and  $-30 R_E$ ; and Figure 6c shows the energetic electron fluxes measured by the LANL 1990-095 geosynchronous satellite. The IMF  $B_z$  is very stable on this day. A large solar wind pressure impulse occurs around 0030 UT and a second and smaller one around 0230 UT. After 0500 UT the solar wind pressure is also very stable. In the bottom panel of Figure 6a the solar wind pressure data are plotted in an expanded scale in order to show fine perturbations. Only some small and irregular variations exist in the solar wind pressure after 0500 UT.

[25] The magnetospheric and ionospheric variations after each substorm onset can be attributed solely to the magne-

tospheric substorm process, because the solar wind is stable. The vertical dotted lines in Figure 6 indicate the substorm onsets identified from the southward turnings of the magnetospheric magnetic field  $B_z$  component measured by Geotail. Huang [2002] has made a detailed analysis of the Geotail measurements in the near tail on 18 April 2002, and the recurrent southward turnings of the magnetospheric magnetic field are interpreted as the signature of periodic magnetic reconnection in the near-Earth neutral line. The sudden increases (injections) of the electron fluxes in Figure 6c show an energy dispersion after 0800 UT and are not exactly coincident with the near-tail reconnection onsets in Figure 6b. This is because the geosynchronous satellite is outside the injection region after 0800 UT, and the particles are injected to the inner magnetosphere near midnight and then drift to the satellite position. Huang *et al.* [2003b] have reported on multiple space-based and ground-based instrumental measurements in the magnetosphere and ionosphere of this case. They show that periodic substorms occur on this day under continuous southward IMF conditions. The generation of the periodic substorms is related to periodic magnetic reconnection in a near-Earth neutral line. The substorm onsets and their periodicity are determined by the magnetosphere, and each substorm does not have to be triggered by either a northward IMF turning or a solar wind pressure impulse. The details of the magnetospheric-ionospheric measurements and interpretation are provided by Huang [2002] and Huang *et al.* [2003b]. What we want to show in Figure 6 is that periodic substorm onsets occur when the IMF  $B_z$  and solar wind pressure are stable.

[26] Figure 7a shows the inner magnetospheric magnetic field  $B_z$  component measured by the GOES 8 satellite.

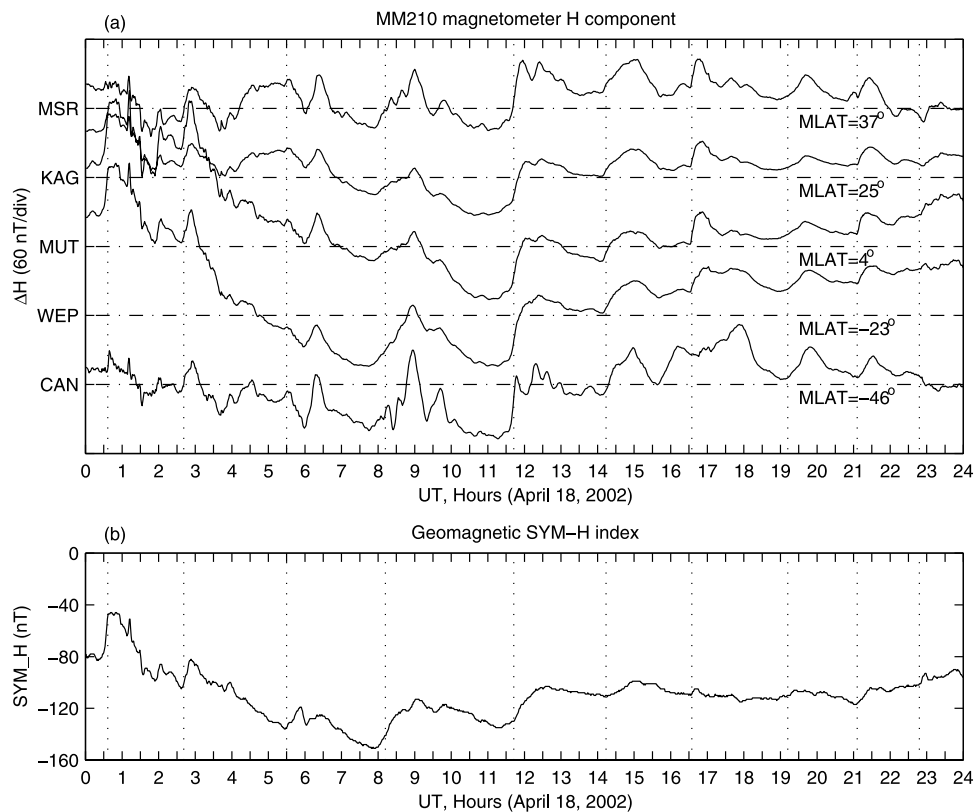


**Figure 8.** (a) Deviations of the  $H$  component of the STEP magnetometers at MSR, KAG, MUT, Weipa (WEP), and Canberra (CAN) and (b) SYM- $H$  index on 18 April 2002.

Figure 7b shows the ionospheric electric field  $E_y$ , measured by the Jicamarca radar and the magnetometer  $H$  component deviations at Piura and Jicamarca. The first sudden change in these measurements at 0036 UT may be related to both the solar wind pressure impulse and a substorm onset. After the second substorm onset at 0241 UT (2141 MLT at Jicamarca) the ionospheric electric field  $E_y$  perturbation is westward (negative), which is consistent with the results in Figure 5d. However, there is an eastward (positive) perturbation in the electric field  $E_y$  after the third substorm onset at 0530 UT (0030 MLT), and it is not clear why the polarity of the electric field perturbation in this event is different from the others. The electric field perturbation is again westward at the onset at 0812 UT (0312 MLT). The variations of the magnetometer  $H$  component at Jicamarca and Piura are not related to the electric field perturbations. For example, the  $H$  deviations increase after each substorm onset, while the electric field  $E_y$  decreases after the onsets at 0036, 0241, and 0812 UT. The  $H$  deviations after the onset at 0530 UT are rather large and could not be produced by the small variation in the electric field. After the onset at 0812 UT the  $H$  deviations are slightly positive, while the electric field perturbation is strongly negative. In addition, the amplitude of the  $H$  deviations is almost the same at Piura and Jicamarca, implying that there is no Cowling electrojet effect enhanced by the electric field.

[27] On the other hand, the ground magnetometer  $H$  deviations are very similar to those in the magnetospheric magnetic field  $B_z$  component at the same local time. In particular, both the GOES 8 satellite and ground magne-

tometer measurements show a small increase between 0241 and 0317 UT, a large increase between 0317 and 0406 UT, a large increase between 0530 and 0620 UT, and a small increase between 0810 and 0900 UT. Similar to those shown in Figure 5d, the nightside ground magnetometer  $H$  deviations are closely correlated with the magnetospheric dipolarization process after substorm onsets. When GOES moves to the dayside, the dipolarization signature becomes much weaker.

[28] The  $H$  deviations of the STEP magnetometers of this case are shown in Figure 8a. The magnetometers over a large latitudinal range between 37° and -46° magnetic latitudes detect an increase after each substorm onset over 24 hours, and the amplitude of the  $H$  deviations does not show significant change in latitude. Note that the IMF  $B_z$  and solar wind pressure are very stable, and the magnetometer  $H$  increases are the response to the substorm onsets. The only exception is the decrease in the  $H$  deviations after the onset at 0530 UT. As shown in Figure 7b, there is an eastward perturbation in the ionospheric electric field measured by the Jicamarca radar on the nightside after 0530 UT. On the dayside the corresponding electric field should be westward. The negative  $H$  deviations in the STEP magnetometers after 0530 UT (~1430 MLT) on the dayside may be related to the westward electric field perturbation.

[29] We plot the SYM- $H$  index on 18 April 2002 in Figure 8b. SYM- $H$  shows an increase (or becomes less negative) after each substorm onset over an interval of 24 hours, and the increase in SYM- $H$  is as large as 20–

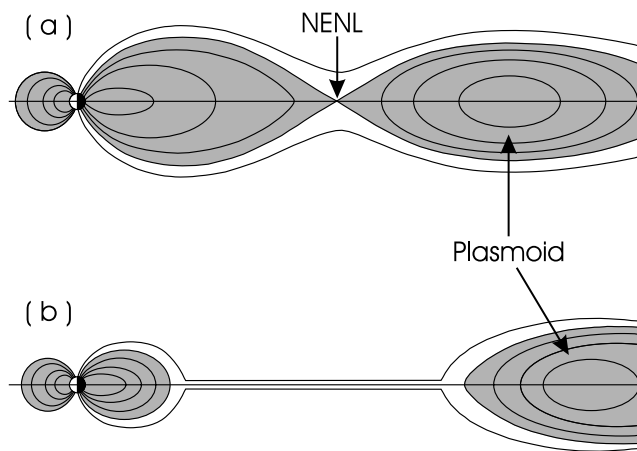


**Figure 9.** Illustration of the magnetospheric magnetic topology (a) at the substorm onset and (b) during the expansion phase. NENL represents the near-Earth neutral line. The volume of the region with closed field lines earthward of the NENL becomes much smaller during the expansion phase.

40 nT. It is not surprising that the variations in  $S\text{YM-}H$  are very similar to those in the STEP magnetometer  $H$  deviations, because  $S\text{YM-}H$  is derived from midlatitude magnetometer measurements.

[30] In all the cases presented in this paper, the ground magnetometer  $H$  component in response to substorm onsets shows a positive deviation (an increase) on both the dayside and the nightside. The nightside  $H$  deviations are closely correlated with the inner magnetospheric magnetic field  $B_z$  component at the same local time but are not determined by the ionospheric electric field perturbations. It appears that the ground geomagnetic  $H$  deviations are related to the magnetospheric dipolarization process during the substorm expansion phase. Magnetic reconnection in a near-Earth neutral line (NENL) is a widely accepted mechanism responsible for the generation of isolated substorms [Hones, 1984; Baker *et al.*, 1996]. Huang [2002] and Huang *et al.* [2003b] have used this mechanism to interpret successfully the generation of periodic substorms on 18 April 2002. After the magnetic reconnection occurs, the tail current is disrupted, and the field dipolarizes. The tail current disruption and field dipolarization will give rise to variations in  $Dst$  [Turner *et al.*, 2000; Reeves *et al.*, 2003]. Perhaps, the increase of  $Dst$  after a substorm onset is the superposition of the effects from the tail current disruption, dipolarization, and ionospheric electric field.

[31] We propose an interpretation of the observational characteristics of the magnetometer  $H$  deviations in response to substorm onsets, using the near-Earth magnetic reconnection as the mechanism for the generation of substorms in the magnetosphere. Figure 9 shows an illustration of the magnetospheric magnetic topology during the process of substorms. At the onset of a substorm a near-Earth neutral line occurs in the tail between  $-20$  and  $-30 R_E$  [Nagai *et al.*, 1998; Huang, 2002; Huang *et al.*, 2003b], as shown in Figure 9a. The magnetic reconnection results in the formation of two regions with closed magnetic field lines. One is earthward of the NENL, and the other (a plasmoid) is tailward of the NENL. During the expansion

phase the closed field line region earthward of the NENL moves toward the Earth, while the plasmoid moves tailward. The magnetospheric magnetic field structure near the Earth becomes nearly dipolar, which is the so-called dipolarization. The scenario depicted in Figure 9 is the same as that proposed originally by Hones [1984].

[32] Here our interest is how the dipolarization process affects the inner magnetosphere and ground magnetic field at low latitudes. All the closed field lines earthward of the NENL move toward the Earth during the expansion phase, and the total magnetic flux enclosed by the outermost closed field line is compressed to a much smaller dipolar region. The total magnetic flux within the closed region is conserved, so the magnetic flux density within the closed field line region becomes much higher. The magnetic field within the entire closed inner magnetosphere, including the ground magnetic field, is greatly increased. As a result, nightside ground magnetometers at middle and low latitudes will detect a sudden increase (a positive bay) after the substorm onset. The observed similarity between the ground magnetometer  $H$  deviations at Jicamarca/Piura and GOES 8 magnetospheric magnetic field  $B_z$  component at the same local time supports this interpretation.

[33] On the dayside it is unclear how significantly the inner magnetosphere will be affected by the dipolarization process. We expect that the dayside magnetic field may also increase but with a smaller amplitude than that on the nightside. The ionospheric electric field may play a role in the dayside magnetic variations in response to substorm onsets. As shown above, the ionospheric electric field caused by substorm onsets is eastward on the dayside. Because of the large conductivity in the dayside ionosphere the eastward electric field will increase the Pedersen current and will produce a northward deviation in the ground magnetic field. This is particularly true in the equatorial ionosphere, since the equatorial electrojet current is greatly enhanced through the Cowling effect.

[34] The nightside ground magnetic field  $H$  component will increase after a substorm onset through the dipolarization of the magnetospheric tail, and the dayside magnetic  $H$  component may also increase during the dipolarization and may be enhanced by the eastward ionospheric electric field. Therefore low-latitude magnetometers at all local times (24 hours) will detect an increase (a positive bay) after a substorm onset. As a consequence, the  $Dst/S\text{YM-}H$  index, which is derived from midlatitude magnetometer measurements, will also show an increase after a substorm onset. During the main phase of magnetic storms, the ring current is rapidly developing and produces a rapid decrease in  $Dst/S\text{YM-}H$ . The dipolarization process may only result in a decrease in the time rate of decrease of  $Dst/S\text{YM-}H$ . This explains the *Iyemori and Rao* [1996] observations that the rate of decrease of  $Dst$  becomes more gentle after substorm onsets during the main phase of storms.

### 3. Discussion

[35] The  $Dst/S\text{YM-}H$  index is the fundamental parameter that is used to describe the strength of the largest magnetospheric-ionospheric disturbances, i.e., magnetic storms. The storm-substorm relationship is one of the most significant issues in space physics. *Siscoe and Petschek* [1997]

used the generalized virial theorem to explain the observations of *Iyemori and Rao* [1996]. *Turner et al.* [2000] calculated the contribution of the tail current to the *Dst* index. In this paper, we have presented the observations of *Dst*/*SYM-H* variations caused by substorm onsets during storm times. On the basis of the observations we have proposed an interpretation of the *Dst*/*SYM-H* increases in response to substorm onsets. We emphasize that the magnetic flux within the closed region earthward of the NENL is conserved during the dipolarization process, so the magnetic flux density (or *B*) is increased. Of course, the dipolarization implies disruption of the tail current and release of the tail magnetic energy. Our interpretation is consistent with previous results [*Siscoe and Petschek*, 1997; *Turner et al.*, 2000; *Reeves et al.*, 2003].

[36] On the other hand, it is necessary to clarify some critical issues from the ionospheric aspect. Since isolated substorms are often related to IMF northward turnings, it is difficult to separate the solar wind effect from the substorm effect in producing ionospheric disturbances. As discussed by *Sibeck et al.* [1998], equatorial magnetic deviations can be caused by solar wind pressure perturbations, IMF reorientations, and substorm activity. In order to rule out the effect of solar wind variations, it is desirable to choose intervals under stable solar wind conditions. The periodic substorms during stable southward IMF provide an excellent opportunity to study the substorm effect on the ionosphere. As shown in this paper, the ionospheric signature of substorm onsets alone is an eastward (westward) electric field perturbation on the dayside (nightside) and a positive bay in the low-latitude ground magnetometer *H* components on both the dayside and the nightside.

[37] In the observations reported by *Fejer et al.* [1979] and *Gonzales et al.* [1979], the ionospheric electric field perturbation after a substorm onset was eastward on the nightside. We emphasize that such an electric field perturbation might be caused by penetration of the interplanetary electric field, rather than by the substorm onset. In their cases the substorm onsets were coincident with northward IMF turnings. The interplanetary electric field after a northward IMF turning is dawnward and will, through penetration, produce a westward electric field perturbation in the dayside ionosphere and an eastward electric field perturbation in the nightside ionosphere. In addition, the overshielding effect after a northward IMF turning will also result in an eastward electric field in the nightside ionosphere [*Kelley et al.*, 1979], no matter whether a substorm onset occurs at the time of the northward IMF turning. Our observations clearly show the difference in the polarity between the penetration interplanetary electric field and the substorm-induced electric field. The ionospheric electric field perturbation solely caused by a substorm onset without IMF reorientations is eastward on the dayside and westward on the nightside.

[38] *Kikuchi et al.* [2000] reported that a negative bay occurred in the dayside low-latitude magnetometer *H* component after a substorm onset. *Sastri et al.* [2001] reported similar results. It is important to point out that the substorm onsets were also coincident with northward IMF turnings in their cases. As discussed above, the penetration of the interplanetary electric field associated with a northward IMF turning generates a westward electric field

perturbation in the dayside ionosphere. The dayside ionospheric conductivity is high, and the electric field can produce large magnetic field deviations. It is the westward ionospheric electric field associated with the IMF northward turning, rather than the substorm onset, that produces the negative bay in the dayside magnetometer *H* component. Figure 3 provides an example of this IMF effect after the substorm onset at 1545 UT on 17 April 2002. The substorm onset alone will cause an increase (a positive bay) in the dayside magnetometer *H* component. *Sastri et al.* [2001] reported on a “rather puzzling” event in which a positive bay occurred in the dayside magnetometer *H* component after a substorm onset. In fact, the “puzzling” phenomenon is the real ionospheric signature of the substorm onset.

[39] The low-latitude magnetometer variations after substorm onsets were often interpreted as the consequence of the ring current [e.g., *Gonzales et al.*, 1979]. Energetic particles are injected into the ring current after substorm onsets, and the ring current will be enhanced. The enhanced ring current will result in a decrease, rather than an increase, of the geomagnetic field *H* component at low latitudes. As we show in this paper, the ground magnetometer *H* component increases on both the dayside and the nightside after substorm onsets when there is no IMF effect involved. The increases in *Dst* and low-latitude magnetometer *H* deviations after substorm onsets are related to the dipolarization of the magnetotail but not to the ring current enhancement.

[40] It is well known that a solar wind pressure impulse will compress the magnetosphere and will result in an increase in the magnetospheric magnetic field [*Sibeck*, 1993] and in the ground magnetometer *H* component [*Russell and Ginskey*, 1995]. The variations of the geomagnetic field *H* component at middle latitudes are proportional to the square root of the solar wind pressure change. *Russell et al.* [1994] performed a model calculation and derived the relationship of  $\Delta H = 18\sqrt{\Delta P_{\text{SW}}}$  near noon and  $\Delta H = 15\sqrt{\Delta P_{\text{SW}}}$  near midnight, where the *H* deviation is measured by nanoteslas and the solar wind pressure variation is measured by nanopascals. The measurements of *Francia et al.* [2001] are consistent with the model. In the case of 18 April 2002 in our paper, there is a solar wind pressure increase of  $\sim 10$  nPa after 0030 UT. The expected *H* deviation at the STEP magnetometers ( $\sim 0930$  MLT) from the formula of *Russell et al.* is  $\sim 50$  nT. As shown in Figure 8a, the *H* deviations at Muntinlupa and Weipa (WEP) indeed increase by  $\sim 50$  nT between 0025 and 0040 UT, consistent with the formula. After 0500 UT the solar wind pressure variations are very small. There are three relatively large solar wind pressure impulses at 0616, 1708, and 2245 UT. There is an increase in the magnetometer *H* component after 0616 UT, which may be the compressional effect of the solar wind pressure impulse. Note that the substorm onset occurs at 0530 UT and is not related to the solar wind pressure impulse and magnetometer *H* increase at 0616 UT. It is also very unlikely that the substorm onset at 1636 UT is related to the solar wind pressure impulse at 1708 UT. The substorm onset at 0812 UT may be somehow related to the small solar wind pressure impulse with an amplitude of  $\sim 0.4$  nPa. The empirical formula gives an estimated *H* deviation of  $\sim 11$  nT, while the measured *H* deviations are  $\sim 50$  nT at



Moshiri and WEP. Furthermore, the substorm onsets at 0530, 1142, 1413, 1912, and 2106 UT are not related to any solar wind pressure enhancements, and the measured  $H$  deviations are as large as 20–50 nT. It is certain that the magnetometer  $H$  deviations at the substorm onsets are not the signature of compressions of the magnetosphere by solar wind pressure impulses.

#### 4. Conclusions

[41] We have presented the observations of magnetospheric and ionospheric disturbances caused by substorms during magnetic storms. Our study focuses on the ionospheric signatures at middle and low latitudes. The objective of this paper is to understand how ionospheric electric and magnetic fields vary in response to substorms and to understand why the  $Dst/SYM-H$  index increases after substorm onsets. We have chosen several cases under different solar wind conditions so that we are able to identify which ionospheric signatures are caused by the solar wind alone and which are caused by substorms alone.

[42] Our study reveals that the disturbances of the low-latitude ionospheric electric field and magnetic fields in response to substorm onsets have the following characteristics. We emphasize that the effects of IMF reorientations have been excluded and that these characteristics are solely caused by substorm onsets. (1) The ionospheric electric field perturbation after the substorm onset is eastward on the dayside and westward on the nightside. (2) The ground magnetometer  $H$  deviations over a large latitudinal range (between  $37^\circ$  and  $-46^\circ$  magnetic latitudes) show an increase (20–50 nT) after each substorm onset, no matter whether the magnetometers are located on the dayside or on the nightside. (3) The nightside magnetometer  $H$  deviations are closely correlated with the variations in the inner magnetospheric magnetic field  $B_z$  component, suggesting that the ground  $H$  deviations may be related to the magnetospheric dipolarization process during the expansion phase of substorms. (4) The nightside magnetometer  $H$  deviations are not caused by the ionospheric electric field. On the dayside the eastward electric field after the substorm onset may make a contribution to the increase of the magnetometer  $H$  component. (5) The  $Dst/SYM-H$  index shows an increase (20–40 nT) after the substorm onset.

[43] We have proposed an interpretation of the increase in the magnetometer  $H$  component and  $Dst/SYM-H$  index in response to substorm onsets. We suggest that the increase in the geomagnetic field  $H$  component at middle and low latitudes is related to the magnetospheric dipolarization process. At the onset of substorms a near-Earth neutral line occurs between  $X_{GSM} = -20$  and  $-30 R_E$ . During the expansion phase, all closed field lines earthward of the NENL move toward the Earth, and the magnetic flux enclosed by the outermost closed field line is compressed to a much smaller dipolar region. Because the total magnetic flux within the closed region is conserved, a very important consequence of the dipolarization is that the magnetic flux density within the closed dipolar region is greatly increased, so the magnetic field within the inner magnetosphere, including the ground magnetic field, is increased. The increase in the ground magnetometer  $H$  component caused by the dipolarization is significant on the nightside and may also occur on the

dayside. The ionospheric electric field produced by the substorm onset is eastward on the dayside, which increases the eastward Pedersen current and the  $H$  component of the geomagnetic field. Therefore the ground magnetometer  $H$  component, as well as the  $Dst/SYM-H$  index, will show an increase on both the dayside and the nightside after substorm onsets.

[44] **Acknowledgments.** Work at MIT Haystack Observatory was supported by an NSF cooperative agreement with Massachusetts Institute of Technology. The Jicamarca Radio Observatory is operated by the Instituto Geofísico del Perú, with support from NSF Cooperative Agreement ATM-9911209 through Cornell University; we thank Oscar Veliz for providing processed data from 150-km echoes and magnetograms from Piura and Jicamarca. Solar-Terrestrial Environment Laboratory, Nagoya University, supports construction of the STEP magnetometer database. The Geotail data are provided by S. Kokubun through DARTS at the Institute of Space and Astronautical Science in Japan. The  $SYM-H$  data are provided by the World Data Center for Geomagnetism at Kyoto University. We acknowledge the CDAWeb for access to the Wind and GOES 8 data.

[45] Lou-Chuang Lee thanks Takashi Kikuchi and David G. Sibeck for their assistance in evaluating this paper.

#### References

- Alexeev, I. I., E. S. Belenkaya, V. V. Kalegaev, Y. I. Feldstein, and A. Grafe (1996), Magnetic storms and magnetotail currents, *J. Geophys. Res.*, *101*, 7737.
- Anderson, D., A. Anghel, K. Yumoto, M. Ishitsuka, and E. Kudeki (2002), Estimating daytime vertical  $E \times B$  drift velocities in the equatorial F-region using ground-based magnetometer observations, *Geophys. Res. Lett.*, *29*(12), 1596, doi:10.1029/2001GL014562.
- Baker, D. N., T. I. Pulkkinen, V. Angelopoulos, W. Baumjohann, and R. L. McPherron (1996), Neutral line model of substorms: Past results and present view, *J. Geophys. Res.*, *101*, 12,975.
- Baumjohann, W., M. Hesse, S. Kokubun, T. Mukai, T. Nagai, and A. A. Petrukovich (1999), Substorm dipolarization and recovery, *J. Geophys. Res.*, *104*, 24,995.
- Blanc, M. (1983), Magnetospheric convection effects at mid-latitudes: 1. Saint-Santin observations, *J. Geophys. Res.*, *88*, 211.
- Buonsanto, M. J., and J. M. Holt (1995), Measurements of gradients in ionospheric parameters with a new nine-position experiment at Millstone Hill, *J. Atmos. Sol. Terr. Phys.*, *57*, 705.
- Buonsanto, M. J., S. A. Gonzalez, G. Lu, B. W. Reinisch, and J. P. Thayer (1999), Coordinated incoherent scatter radar study of the January 1997 storm, *J. Geophys. Res.*, *104*, 24,625.
- Clauer, C. R., and R. L. McPherron (1974), Mapping the local time-universal time development of magnetospheric substorms using midlatitude magnetic observations, *J. Geophys. Res.*, *79*, 2811.
- Ebihara, Y., and M. Ejiri (2000), Simulation study on fundamental properties of the storm-time ring current, *J. Geophys. Res.*, *105*, 15,483.
- Fejer, B. G., C. A. Gonzales, D. T. Farley, M. C. Kelley, and R. F. Woodman (1979), Equatorial electric fields during magnetically disturbed conditions: 1. The effect of the interplanetary magnetic field, *J. Geophys. Res.*, *84*, 5797.
- Fejer, B. G., et al. (1990), Low- and mid-latitude ionospheric electric fields during the January 1984 GISMOS campaign, *J. Geophys. Res.*, *95*, 2367.
- Francia, P., S. Lepidi, P. Di Giuseppe, and U. Villante (2001), Geomagnetic sudden impulses at low latitude during northward interplanetary magnetic field conditions, *J. Geophys. Res.*, *106*, 21,231.
- Gonzales, C. A., M. C. Kelley, B. G. Fejer, J. F. Vickrey, and R. F. Woodman (1979), Equatorial electric fields during magnetically disturbed conditions: 2. Implications of simultaneous auroral and equatorial measurements, *J. Geophys. Res.*, *84*, 5803.
- Hones, E. W., Jr. (1984), Plasma sheet behavior during substorms, in *Magnetic Reconnection in Space and Laboratory Plasmas*, *Geophys. Monogr. Ser.*, vol. 30, edited by E. W. Hones Jr., p. 178, AGU, Washington, D. C.
- Huang, C.-S. (2002), Evidence of periodic (2–3 hour) near-tail magnetic reconnection and plasmoid formation: Geotail observations, *Geophys. Res. Lett.*, *29*(24), 2189, doi:10.1029/2002GL016162.
- Huang, C.-S., and J. C. Foster (2001), Variations of midlatitude ionospheric plasma density in response to an interplanetary shock, *Geophys. Res. Lett.*, *28*, 4425.
- Huang, C.-S., J. C. Foster, and P. E. Erickson (2002), Effects of solar wind variations on the midlatitude ionosphere, *J. Geophys. Res.*, *107*(A8), 1192, doi:10.1029/2001JA009025.

- Huang, C.-S., J. C. Foster, L. P. Goncharenko, G. J. Sofko, J. E. Borovsky, and F. J. Rich (2003a), Midlatitude ionospheric disturbances during magnetic storms and substorms, *J. Geophys. Res.*, *108*(A6), 1244, doi:10.1029/2002JA009608.
- Huang, C.-S., J. C. Foster, G. D. Reeves, G. Le, H. U. Frey, C. J. Pollock, and J.-M. Jahn (2003b), Periodic magnetospheric substorms: Multiple space-based and ground-based instrumental observations, *J. Geophys. Res.*, *108*(A11), 1411, doi:10.1029/2003JA009992.
- Huang, C.-S., G. D. Reeves, J. E. Borovsky, R. M. Skoug, Z. Y. Pu, and G. Le (2003c), Periodic magnetospheric substorms and their relationship with solar wind variations, *J. Geophys. Res.*, *108*(A6), 1255, doi:10.1029/2002JA009704.
- Iyemori, T., and D. R. K. Rao (1996), Decay of the Dst field of geomagnetic disturbance after substorm onset and its implication to storm-substorm relation, *Ann. Geophys.*, *14*, 618.
- Kelley, M. C., B. G. Fejer, and C. A. Gonzales (1979), An explanation for anomalous ionospheric electric fields associated with a northward turning of the interplanetary magnetic field, *Geophys. Res. Lett.*, *6*, 301.
- Kelley, M. C., J. J. Makela, J. L. Chau, and M. J. Nicolls (2003), Penetration of the solar wind electric field into the magnetosphere/ionosphere system, *Geophys. Res. Lett.*, *30*(4), 1158, doi:10.1029/2002GL016321.
- Kikuchi, T., H. Luhr, K. Schlegel, H. Tachihara, M. Shinohara, and T. I. Kitamura (2000), Penetration of auroral electric fields to the equator during a substorm, *J. Geophys. Res.*, *105*, 23,251.
- Kikuchi, T., S. Tsunomura, K. Hashimoto, and K. Nozaki (2001), Field-aligned current effects on midlatitude geomagnetic sudden commencements, *J. Geophys. Res.*, *106*, 15,555.
- Kikuchi, T., K. K. Hashimoto, T. I. Kitamura, H. Tachihara, and B. J. Fejer (2003), Equatorial counter-electrojets during substorms, *J. Geophys. Res.*, *108*(A11), 1406, doi:10.1029/2003JA009915.
- Kitamura, K., H. Kawano, S.-I. Ohtani, A. Yoshikawa, K. Yumoto, and the CPMN Group (2003), Quasi-periodic substorms during recovery phase of magnetic storm for space weather study, paper presented at International Symposium on Information Science and Electrical Engineering 2003, Fukuoka, Japan, 13–14 Nov.
- Kudeki, E., and C. D. Fawcett (1993), High resolution observations of 150 km echoes at Jicamarca, *Geophys. Res. Lett.*, *20*, 1987.
- Lyons, L. R. (1995), A new theory for magnetospheric substorms, *J. Geophys. Res.*, *100*, 19,069.
- Maltsev, Y. P., A. A. Arykov, E. G. Belova, B. B. Gvozdevsky, and V. V. Safargaleev (1996), Magnetic flux redistribution in the storm time magnetosphere, *J. Geophys. Res.*, *101*, 7697.
- McPherron, R. L. (1997), The role of substorms in the generation of magnetic storms, in *Magnetic Storms*, *Geophys. Monogr. Ser.*, vol. 98, edited by B. T. Tsurutani et al., p. 131, AGU, Washington D. C.
- McPherron, R. L., T. Terasawa, and A. Nishida (1986), Solar wind triggering of substorm expansion onset, *J. Geomag. Geoelectr.*, *38*, 1089.
- Nagai, T., M. Fujimoto, Y. Saito, S. Machida, T. Terasawa, R. Nakamura, T. Yamamoto, T. Mukai, A. Nishida, and S. Kokubun (1998), Structure and dynamics of magnetic reconnection for substorm onsets with Geotail observations, *J. Geophys. Res.*, *103*, 4419.
- Nishida, A. (1968), Coherence of geomagnetic DP 2 fluctuations with interplanetary magnetic variations, *J. Geophys. Res.*, *73*, 5549.
- Reeves, G. D., et al. (2003), IMAGE, POLAR, and geosynchronous observations of substorm and ring current ion injection, *Disturbances in Geospace: The Storm-Substorm Relationship*, *Geophys. Monogr. Ser.*, vol. 142, edited by A. S. Sharma, Y. Kamide, and G. S. Lakhina, p. 91, AGU, Washington, D. C.
- Russell, C. T., and M. Ginsky (1995), Sudden impulses at subauroral latitudes: Response for northward interplanetary magnetic field, *J. Geophys. Res.*, *100*, 23,695.
- Russell, C. T., M. Ginsky, and S. M. Petrinec (1994), Sudden impulses at low-latitude stations: Steady state response for northward interplanetary magnetic field, *J. Geophys. Res.*, *99*, 253.
- Sastri, J. H., J. V. S. V. Rao, D. R. K. Rao, and B. M. Pathan (2001), Daytime equatorial geomagnetic H component response to the growth phase and expansion phase onset of isolated substorms: Case studies and their implications, *J. Geophys. Res.*, *106*, 29,925.
- Sibeck, D. G. (1993), Transient magnetic field signatures at high latitudes, *J. Geophys. Res.*, *98*, 243.
- Sibeck, D. G., K. Takahashi, K. Yumoto, and G. D. Reeves (1998), Concerning the origin of signatures in dayside equatorial ground magnetometers, *J. Geophys. Res.*, *103*, 6763.
- Siscoe, G. L., and H. E. Petschek (1997), On storm weakening during substorm expansion phase, *Ann. Geophys.*, *15*, 211.
- Turner, N. E., D. N. Baker, T. I. Pulkkinen, and R. L. McPherron (2000), Evaluation of the tail current contribution to Dst, *J. Geophys. Res.*, *105*, 5431.
- Yumoto, K., and the CPMN Group (2001), Characteristics of Pi 2 magnetic pulsations observed at the CPMN stations: A review of the STEP results, *Earth Planets Space*, *53*, 981.

J. L. Chau, Radio Observatorio de Jicamarca, Instituto Geofisico del Peru, Apartado 13-0207, Lima, Peru. (chau@geo.igp.gob.pe)

J. C. Foster, L. P. Goncharenko, and C.-S. Huang, Haystack Observatory, Massachusetts Institute of Technology, Route 40, Westford, MA 01886, USA. (jcf@haystack.mit.edu; lpg@haystack.mit.edu; cshuang@haystack.mit.edu)

K. Kitamura and K. Yumoto, Space Environment Research Center, Kyushu University 33, 6-10-1 Hakozaki, Fukuoka 812-8581, Japan. (kitaken@serc.kyushu-u.ac.jp; yumoto@geo.kyushu-u.ac.jp)

G. D. Reeves, Los Alamos National Laboratory, NIS-1 MS D-466, Los Alamos, NM 87545, USA. (reeves@lanl.gov)